ELSEVIER

Journal of Organometallic Chemistry 528 (1997) 47–58

Journal of Organometallic Chemistry

Synthesis, characterisation and structure of a strained ring-tilted bis(indenyl)iron complex [1]

Francisco Martinez Alías [a], Stephen Barlow [a], Jonathan S. Tudor [a], Dermot O'Hare [a,*], Randall T. Perry [b], James M. Nelson [b], Ian Manners [b]

[a] *Inorganic Chemistry Laboratory, University of Oxford, South Parks Road, Oxford OX1 3QR, UK*
[b] *Department of Chemistry, University of Toronto, 80 St. George Street, Toronto, Ont. M5S 3H6, Canada*

Received 26 March 1996; in revised form 27 April 1996

Abstract

The new bridged ligand $(C_9Me_6H)_2SiMe_2$ **9** has been prepared and used to synthesise the first strained *ansa*-bridged bis(indenyl)iron complex $Fe(\eta^5\text{-}C_9Me_6)_2SiMe_2$ **11**. The properties of **11** are compared with those of other $SiMe_2$-bridged [1]-ferrocenophanes and with the unbridged analogue $Fe(\eta^5\text{-}C_9Me_6H)_2$ **8**. UV–vis and ^{13}C NMR data are consistent with a ring-tilted structure for **11**; the strain in the molecule is demonstrated by the observation of alcoholysis and hydrolysis products in its FAB mass spectrum. The crystal structure of *rac*-$Fe(\eta^5 - C_9Me_6)_2SiMe_2$ **11a** has been determined; the ring tilt angles of 13.0 and 13.8° (for the two independent molecules in the cell) are the lowest so far reported for a silicon-bridged [1]-ferrocenophane, whilst the distortion of the bridgehead atoms from ideal sp^2 geometry is reflected in the angles β between the planes of the five-membered indenyl rings and the C–Si bonds of 43.1 and 41.2°. ^{57}Fe Mössbauer spectra of **11a** and **8** suggest the presence of Fe–Si interactions in the former compound.

Keywords: Iron; Indenyl; Crystal structure; Metallocene; *Ansa*-bridged; Mössbauer

1. Introduction

The first [1]-ferrocenophanes were reported in 1975 by Osborne and Whiteley [1]. Stoichiometric ring-opening reactions between nucleophiles and [1]-ferrocenophanes were first reported in 1979 by Fischer et al. [2]; they reported the methanolysis and hydrolysis products of $Fe(\eta^5\text{-}C_5H_4)_2SiMe_2$ **1** and used the ring-opening reaction to functionalise surfaces with ferrocenyl groups. Other ring-opening reactions of phosphorus-bridged [1]-ferrocenophanes with alkyl and aryl lithium reagents were reported in 1982 by Seyferth's group [3,4]; they also used small ratios of nucleophile to ferrocenophane in attempts to form polymers, but only obtained short chain oligomers. In 1992 thermal ring-opening polymerisation (TROP) of [1]-ferrocenophanes was reported (Scheme 1) [5,6]. The resulting polymers are unusual among transition-metal-containing polymers in that the organometallic moieties form part of the main chain of the polymer, rather than being pendant groups, as in, for example, poly(vinylferrocene). A variety of silicon-bridged [1]-ferrocenophanes has been synthesised and many have been successfully polymerised. These species have had a wide variety of substituents on the bridging atom [7–12], thus allowing a wide variation in the properties of the resulting polymers. We have recently described the synthesis and properties of a series of ring-methylated $SiMe_2$-bridged [1]-ferrocenophanes (Fig. 1) [13,14] and their ring-opened polymers [15]. Their structural and spectroscopic properties show a number of interesting trends. The reaction has also been extended to germanium [16,17], phosphorus [18], and sulphur-bridged species [19], as well as to

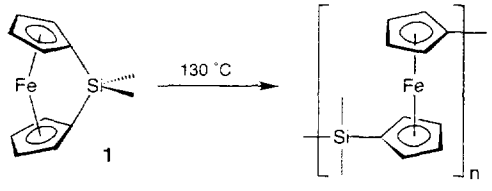

1

Scheme 1. Thermal ring opening polymerisation of a [1]-ferrocenophane.

* Corresponding author.

[1] Dedicated to Professor M.L.H. Green on the occasion of his sixtieth birthday.

SSDI 0022-328X(96)06434-0

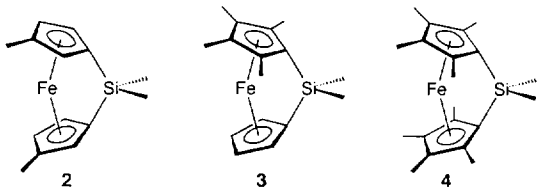

Fig. 1. Some ring-methylated $SiMe_2$-bridged [1]-ferrocenophanes.

[2]-ferrocenophanes [20] and [2]-ruthenocenophanes [21] with hydrocarbon bridges.

The ROP reaction has also been achieved at ambient temperature by the use of anionic initiators [22,23] γ-radiation [24] or catalytic amounts of certain late transition metal compounds [25,26]. The first of these three alternative routes is especially powerful as it permits chain length control, end group control and the formation of block copolymers with other organic, inorganic or organometallic monomers [22,23].

Here we report the synthesis of the first ring-tilted dibenzo-[1]-ferrocenophane, i.e. an *ansa*-bridged bis(indenyl)iron complex, the properties and crystal structure of which provide interesting comparison with the species shown in Scheme 1 and Fig. 1.

2. Experimental details

2.1. Instrumental methods

Elemental analyses were performed by the analytical department of the Inorganic Chemistry Laboratory, Oxford. Solution NMR spectra were recorded using a Bruker AM 300 or a Varian Unity Plus 500 spectrometer. Spectra were referenced via the residual protiosolvent; chemical shifts (δ) are quoted in parts per million relative to Me_4Si at 0 ppm. Low resolution electron impact (EI) mass spectra were recorded in the Inorganic Chemistry Laboratory using an AEI MS 9802 instrument calibrated with perfluorokerosene. Low resolution FAB mass spectra were recorded by the EPSRC Mass Spectrometry Service, University of Wales, Swansea with a VG Autospec instrument using caesium ion bombardment at 25 kV onto a 3-nitrobenzyl alcohol matrix of the sample. UV–vis data were recorded on dry THF solutions using a Hewlett-Packard 6452A diode array instrument with a 1 cm cell. Room temperature ^{57}Fe Mössbauer data were obtained using a Ranger Scientific Inc. Vt-1200 instrument with an MS-1200 digital channel analyser. An Amersham 6-mCi ^{57}Co γ-ray source was employed. Spectra were referenced to iron foil. Cyclic voltammograms were recorded using a platinum working, tungsten auxillary and silver wire pseudo-reference electrode. Measurements were made under argon on deoxygenated dry dichloromethane solutions, ca. 5×10^{-4} M in the sample and 0.1 M in $^{n}Bu_4N^+PF_6^-$. Potentials were referenced to the ferrocenium/ferrocene couple at 0 V by addition of ferrocene to the cell. The reversibility of redox processes was judged by comparison with the behaviour of the ferrocenium/ferrocene couple under the same conditions.

2.2. General considerations

Operations involving oxygen- or water-sensitive materials were carried out under nitrogen or in vacuo using standard Schlenk techniques or a Vacuum Atmospheres glove-box. Where necessary solvents were dried by reflux over either sodium–potassium alloy (pentane, petroleum ether (b.p. 40–60°C)), potassium (THF) or P_2O_5 (dichloromethane). These solvents were distilled under nitrogen and stored under nitrogen over activated type 4 Å molecular sieves. Solvents were deoxygenated prior to use by passage of a stream of nitrogen through the solvent. C_6D_6 was dried by reflux over molten potassium and purified by trap-to-trap distillation. Silicon tetrachloride (Aldrich) was purified by distillation. TMEDA was purified by distillation from CaH_2. 2,3,4,5,6,7-Hexamethylindanone **5** was prepared as described previously [27]. Methyllithium and n-butyllithium solutions were supplied by Aldrich. $FeCl_2 \cdot 1.5THF$ was prepared by Soxhlet extraction of anhydrous $FeCl_2$, prepared by dehydration of $FeCl_2 \cdot 4H_2O$ at 200°C in vacuo, into THF.

2.3. Preparation of $C_9Me_6H_2$, 6

A solution of **1** (55 g, 0.254 mol) in diethyl ether (50 ml) was added dropwise to a stirred slurry of $LiAlH_4$ (3.21 g, 0.085 mol) in diethyl ether (150 ml) at 0°C over a period of 1 h. After 8 h, water (100 ml) was cautiously added to the mixture. 10% phosphoric acid (100 ml) was added to dissolve the precipitated inorganics. The organic phase was separated and the aqueous phase washed with diethyl ether (3×30 ml). The combined organic layers were then stirred over 85% phosphoric acid (30 ml) for 12 h. The organic phase was separated and the aqueous layer washed with diethyl ether (3×30 ml). The combined organics were washed with saturated Na_2CO_3 solution and dried over $MgSO_4$; solvent removal followed by recrystallisation from cold methanol gave **6** as a white solid (41 g, 81%). ^{1}H NMR ($CDCl_3$): δ 1.25 (d, $J = 7.3$ Hz, 3H, $CHCH_3$), 2.02 (s, 3H, CH_3), 2.20 (apparent s, 6H, CH_3), 2.28 (s, 3H, CH_3), 2.29, (s, 3H, CH_3), 3.25 (q, $J = 7.3$ Hz, 1H, $CHCH_3$), 6.46 (s, 1H, vinyl CH). ^{13}C{^{1}H} NMR ($CDCl_3$): δ 15.0 (CH_3), 15.7 ($2 \times CH_3$), 15.9 (CH_3), 16.1 (CH_3), 16.5 (CH_3), 42.5 ($CHCH_3$), 124.3 (vinyl CH), 125.2 (quat.), 128.8 (quat.), 130.8 (quat.), 133.2 (quat.), 140.7 (quat.), 144.8 (quat.), 149.4 (quat.). MS (EI, room temp.): m/z 200 (M^+, 64%), 185 (M^+–Me, 96%), 170 (M^+–2Me, 25%), 155 (M^+–3Me, 31%), 140 (M^+–4Me, 23%).

2.4. Preparation of C_9Me_6HLi, 7

^{n}BuLi (112 ml of 2.5 M solution in hexanes) was added dropwise to a solution of **6** (48.5 g, 0.24 mol) and TMEDA (12 ml, 0.24 mol) in 200 ml of petroleum ether (b.p. 40–60°C) at 0°C. After 12 h, the resulting pale yellow precipitate was collected on a frit and washed with 3 × 30 ml petroleum ether (b.p. 40–60°C). The off white solid (48.8 g, 97%) was then dried in vacuo.

2.5. Preparation of $Fe(\eta^5\text{-}C_9Me_6H)_2$, 8

A solution of **7** (1.00 g, 4.85 mmol) in 20 ml THF was added slowly to a slurry of $FeCl_2 \cdot 1.5THF$ (0.61 g, 2.60 mmol) in 20 ml THF at room temperature to afford a deep purple solution. After 12 h the solvent was removed in vacuo and the resulting residue extracted with petroleum ether (b.p. 40–60°C). The purple extracts were filtered through a bed of Celite, concentrated and cooled to −30°C; the resulting solids washed with cold petroleum ether (b.p. 40–60°C) and dried in vacuo to afford a purple powder (0.71 g, 65%) which NMR spectroscopy revealed to be an approximately 1 : 1 mixture of the two diastereomers of **8**. Anal. Found: C, 78.7; H, 8.3. $C_{30}H_{38}Fe$ Calc.: C, 79.3; H, 8.8%. ^{1}H NMR (C_6D_6): δ 1.77 (2 × s, 12H, CH_3), 1.86 (s, 6H, CH_3), 1.88 (s, 6H, CH_3), 2.04 (s, 6H, CH_3), 2.07 (s, 6H, CH_3), 2.09 (s, 6H, CH_3), 2.15 (2 × s, 12H, CH_3), 2.16 (s, 6H, CH_3), 2.23 (s, 6H, CH_3), 2.31 (s, 6H, CH_3), 4.06 (2 × s, 4H, C_9Me_6H). ^{13}C{^{1}H} NMR (C_6D_6): δ 11.9 (*C*H_3), 12.5 (*C*H_3), 12.8 (*C*H_3), 13.1 (*C*H_3), 16.3 (*C*H_3), 16.4 (*C*H_3), 16.5 (*C*H_3), 16.6 (*C*H_3), 16.8 (2 × *C*H_3), 16.9 (*C*H_3), 17.0 (*C*H_3), 60.8 (*C*H), 60.9 (*C*H), 72.6 (2 × Fe*C* quat.), 84.1 (Fe*C* quat.), 84.8 (Fe*C* quat.), 85.1 (Fe*C* quat.), 85.4 (Fe*C* quat.), 87.3 (Fe*C* quat.), 87.9 (Fe*C* quat.), 127.9 (benzenoid quat.), 128.1 (benzenoid quat.), 128.3 (benzenoid quat.), 128.4 (benzenoid quat.), 128.8 (benzenoid quat.), 128.9 (benzenoid quat.), 130.0 (benzenoid quat.), 131.1 (benzenoid quat.). MS (EI, 200°C): *m/z* 455 (M^+, 40%), 440 (M^+–Me, 3%). UV – vis: λ_{max} (ε) 235 (6680×10^3), 285 (3750×10^3), 425 (477×10^3), 550 (271×10^3) nm (mol^{-1} cm^2).

2.6. Preparation of $(C_9Me_6H)_2SiMe_2$, 9

$SiCl_4$ (3.2 ml, 28 mmol) in THF (50 ml) was added dropwise to a stirred suspension of **7** (11.5 g, 55.9 mmol) in THF (200 ml) at −78°C. The reaction mixture was allowed to warm slowly to room temperature and then left to stir for a further 12 h. The solution was then recooled to −78°C and treated dropwise with MeLi (100 ml, 1.12 M solution in diethyl ether), allowed to warm slowly to room temperature and then stirred for a further 12 h. The mixture was again cooled to −78°C and degassed methanol (3.7 ml) added by syringe. The reaction mixture was allowed to warm to room temperature; the solvent was then removed in vacuo and the solid residue was extracted into hot toluene. The solution was filtered through Celite; concentration and cooling to −30°C gave a white solid, *rac*-$(C_9Me_6H)_2SiMe_2$ **9a** (4.48 g, 35%). Anal. Found: C, 83.6; H, 10.0. $C_{32}H_{44}Si$ Calc.: C, 84.1; H, 9.7%. ^{1}H NMR (C_6D_6): δ −0.39 (s, 6H, SiCH_3), 2.13 (s, 6H, indenyl CH_3), 2.14 (s, 6H, indenyl CH_3), 2.17 (s, 6H, indenyl CH_3), (s, 6H, indenyl CH_3), 2.27 (s, 6H, indenyl CH_3), 2.49 (s, 6H, indenyl CH_3); 3.67 (s, 2H, C*H*). ^{13}C NMR (C_6D_6): δ −3.6 (Si*C*H_3), 15.2 (indenyl *C*H_3), 15.9 (indenyl *C*H_3), 16.3 (indenyl *C*H_3), 16.4 (indenyl *C*H_3), 19.1 (indenyl *C*H_3), 47.4 (*C*H), 126.2 (quat.), 126.8 (quat.), 129.7 (quat.), 132.1 (quat.), 133.1 (quat.), 139.3 (quat.), 141.9 (quat.), 142.6 (quat.). Further concentration and cooling of the supernatant afforded *meso*-$(C_9Me_6H)_2SiMe_2$ **9b**. Yield 3.84 g (30%). ^{1}H NMR (C_6D_6): δ −0.38 (s, 3H, SiCH_3); −0.30 (s, 3H, SiCH_3); 1.89 (s, 6H, indenyl CH_3); 2.16 (s, 6H, indenyl CH_3); 2.17 (s, 6H, indenyl CH_3); 2.18 (s, 6H, indenyl CH_3); 2.21 (s, 6H, indenyl CH_3); 2.48 (s, 6H, indenyl CH_3); 3.56 (s, 2H, C*H*). ^{13}C NMR (C_6D_6): δ −2.5 (Si*C*H_3), −1.5 (Si*C*H_3), 15.3 (indenyl *C*H_3), 16.3 (2 × indenyl *C*H_3), 16.4 (indenyl *C*H_3), 19.0 (indenyl *C*H_3), 47.4 (*C*H), 126.2 (quat.), 127.0 (quat.), 128.3 (quat.), 128.7 (quat.), 132.2 (quat.), 139.9 (quat.), 143.0 (quat.) (remaining quat. obscured). MS (FAB): *m/z* 456 (M^+, 15%), 257 (M^+–C_9Me_6H, 100%), 199 ($C_9Me_6H^+$, 44%).

2.7. Preparation of $(C_9Me_6Li)_2SiMe_2$, 10

^{n}BuLi (12 ml, 2.5 M solution in hexanes) was added dropwise to a solution of **9b** (6.00 g, 13.12 mmol) and TMEDA (4 ml, 26.2 mmol) in 200 ml petroleum ether (b.p. 40–60°C). After 12 h the resulting yellow precipitate was collected on a frit and then washed with pentane (3 × 30 ml) and dried in vacuo to yield **10** (5.95 g, 96%).

2.8. Preparation of $Fe(\eta^5\text{-}C_9Me_6)_2SiMe_2$, 11

A solution of **10** (0.97 g, 2.03 mmol) in THF (20 ml) was added dropwise to a stirred slurry of $FeCl_2 \cdot 1.5THF$ (0.52 g, 2.21 mmol) in THF (20 ml) at 0°C. After stirring for 12 h, the solvent was removed under vacuum and the solid residue extracted into pentane. The extracts were filtered through Celite, concentrated and cooled to afford an isomeric mixture of **11** as red microcrystals (0.2 g, 20%) which were washed with cold pentane and dried in vacuo. Single crystals of the pure isomer **11a** were obtained by slow recrystallisation from pentane. Anal. Found: C, 75.1; H, 8.7. $C_{32}H_{42}FeSi$ Calc.: C, 75.3; H, 8.3%. ^{1}H NMR (C_6D_6): δ for **11a**, 1.14 (s, 6H, SiCH_3), 1.23 (s, 6H, indenyl CH_3), 1.45

(s, 6H, indenyl CH_3), 1.97 (s, 6H, indenyl CH_3), 2.12 (s, 6H, indenyl CH_3), 2.34 (s, 6H, indenyl CH_3), 2.50 (s, 6H, indenyl CH_3); δ for **11b**, 0.98 (s, 3H, SiCH_3), 1.15 (s, 3H, SiCH_3), 1.66 (s, 6H, indenyl CH_3), 1.73 (s, 6H, indenyl CH_3), 1.79 (s, 6H, indenyl CH_3), 2.14 (s, 6H, indenyl CH_3), 2.15 (s, 6H, indenyl CH_3), 2.16 (s, 6H, indenyl CH_3). $^{13}C\{^1H\}$ NMR (C_6D_6): δ for **11a**, 8.6 (Si CH_3), 11.5 (indenyl CH_3), 11.9 (indenyl CH_3), 16.3 (indenyl CH_3), 17.28 (indenyl CH_3), 17.5 (indenyl CH_3), 21.7 (*ipso* CFe), 22.9 (indenyl CH_3), 83.5 (CFe), 93.0 (CFe); 93.8 (CFe); 99.0 (CFe); 129.5 (benzenoid quat.), 130.8 (benzenoid quat.), 131.9 (benzenoid quat.), 132.7 (benzenoid quat.); δ for **11b**, 5.9 (Si CH_3), 8.6 (SiCH$_3$), 11.3 (indenyl CH_3), 12.7 (indenyl CH_3), 13.7 (indenyl CH_3), 16.5 (indenyl CH_3), 17.0 (indenyl CH_3), 20.3 (*ipso* CFe), 22.6 (indenyl CH_3), 83.5 (CFe), 92.3 (CFe); 93.5 (CFe), 99.6 (CFe), 128.4 (benzenoid quat.), 130.5 (benzenoid quat.), 132.7 (benzenoid quat.), (remaining quat. obscured). MS (FAB): *m/z* 1038 ({Fe(C_9Me_6H)(C_9Me_6-$SiMe_2$)}$_2$O), 9%), 663 (Fe(C_9Me_6H)($C_9Me_6SiMe_2$-$OC_6H_4NO_2$), 100%), 647 (Fe(C_9Me_6H)($C_9Me_6SiMe_2$-OC_6H_4NO), 9%), 528 (Fe(C_9Me_6H)($C_9Me_6SiMe_2OH$), 60%), 510 (M+, 7%). UV–vis: λ_{max} (ε) 240 (9080×10^3), 280 (3180×10^3), 470 (648×10^3), 550 (393×10^3) nm (mol^{-1} cm^2).

2.9. Crystal structure determination

Room temperature diffraction data were collected on an Enraf-Nonius CAD4 diffractometer using graphite-monochromated Mo Kα radiation, employing ω–2θ scans. Corrections were made for Lorentz and polarisation effects. The structure was solved by direct methods using SIR92 [28] and refined against F using full-matrix least-squares. Hydrogen atoms were fixed in geometrically idealised positions and given isotropic thermal parameters which were not refined. An absorption correction was applied using DIFABS (max 1.15, min 0.90) [29]. A Chebyshev weighting scheme [30] was applied in the refinement and corrections for the effects of anomalous dispersion and isotropic extinction (via an overall extinction parameter −37.97(1)) [32] were made in the final stages of refinement. All crystallographic calculations were performed using the Oxford CRYSTALS system [32] run on a Silicon Graphics Indigo R3000 computer. Further details are given in Table 1.

3. Results and discussion

3.1. Synthesis

Most [1]-ferrocenophanes have been prepared from 1,1′-dilithioferrocene or its substituted derivatives; alternatively preformed bridged ligands may be reacted with iron(II) salts. The reaction of $(C_5H_4Li)_2SiMe_2$ with iron(II) chloride gives a dimeric species (plus oligomers) rather than the [1]-ferrocenophane [33–35]; however, we have recently reported that **3** and **4** (Fig. 1) may be obtained from the reaction of the corresponding dilithium salt and iron(II) chloride [13], although in the first reaction the yield is low and large quantities of oligomeric material are formed as side-products. The preformed ligand strategy has also been used to obtain strained [2]-metallocenophanes [20,21,36]. Since no dimetallated bis(indenyl)iron species are known, we adopted the preformed ligand route in our quest to prepare a strained dibenzo-[1]-ferrocenophane. Furthermore, we reasoned (by analogy with the reactions of bridged cyclopentadienyl ligands) that this reaction might be more successful if a permethylated ligand was used. We therefore devised the synthesis shown in Scheme 2. Compound **5** was readily converted to hexamethylindene by reduction with lithium aluminum hydride. Surprisingly, work-up with concentrated hydrochloric acid gave 1-chloro-2,3-dihydro-2,3,4,5,6,7-hexamethylindene rather than hexamethylindene. However, the chlorine compound loses HCl and can be readily converted to 1,2,4,5,6,7-hexamethylindene by stirring in refluxing dichloromethane. Use of phosphoric acid in place of HCl was found to afford 1,2,4,5,6,7-hexamethylindene directly.

Table 1
Details of crystal data, data collection, structure solution and refinement for compound **11a**

Formula	$C_{32}H_{42}FeSi$
Molecular mass	510.62
Crystal appearance	dark red block
Crystal size (mm^3)	0.3×0.5×0.6
a (Å)	18.905(4)
b (Å)	13.746(2)
c (Å)	16.033(3)
α (°)	139.95(2)
β (°)	92.47(2)
γ (°)	92.90(2)
V (Å^3)	2655(1)
Crystal class	triclinic
Space group	$P\bar{1}$
Z	4 (two independent molecules)
F(000)	1096
d_{calc} (g cm^{-3})	1.277
μ (Mo Kα) (mm^{-1})	0.629
Reflections measured	6684
Independent reflections	5642
Reflections with $I > 3\sigma(I)$	3281
θ range (°)	0–21
Variables	616
R	0.050
R_w	0.053
S	1.108
$\Delta\rho_{max}$ (e Å^{-3})	0.34
$\Delta\rho_{min}$ (e Å^{-3})	−0.31

The preparation of the silicon-bridged ligand $(C_9Me_6H)_2SiMe_2$ **9** was adapted from a synthesis of $(C_5Me_4H)_2SiMe_2$ previously described by Marks and coworkers [37,38]. The intermediate $(C_9Me_6H)_2SiCl_2$ may be isolated but this gives no improvement in the yield of **9**. Compound **9** is formed as a mixture of diastereomers which differ in their solubilities and ease of lithiation: the more soluble *meso*-$(C_9Me_6H)_2SiMe_2$ **9b** may be readily converted to the dilithium salt **10** by treatment with ^nBuLi in petroleum ether in the presence

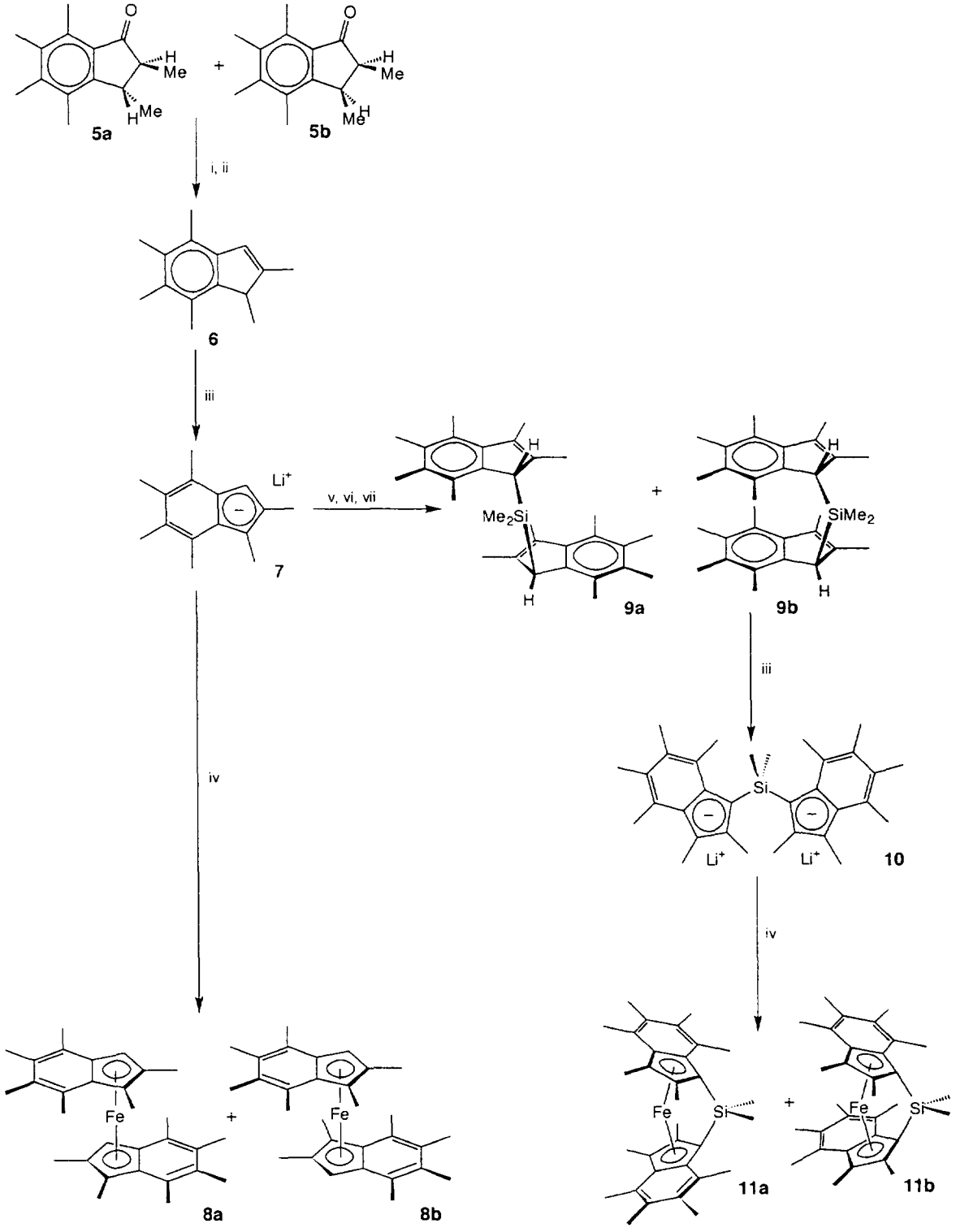

Scheme 2. Reagents and conditions: (i) $LiAlH_4$, Et_2O; (ii) c. H_3PO_4; (iii) ^nBuLi, TMEDA, petroleum ether (b.p. 40–60°C); (iv) $FeCl_2 \cdot 1.5THF$, THF; (v) $SiCl_4$, THF; (vi) MeLi, THF/Et_2O; (vii) MeOH.

of TMEDA, whereas we have not been able to cleanly dilithiate *rac*-$(C_9Me_6H)_2SiMe_2$ **9a**.

$Fe(\eta^5\text{-}C_9Me_6)_2SiMe_2$ **11** was formed in low yield from the reaction of $(LiC_9Me_6)_2SiMe_2$ **10** and $FeCl_2 \cdot 1.5THF$ as a mixture of the two possible diastereomers. The two isomers can readily be distinguished by the number of SiMe resonances in the ^1H or ^{13}C NMR spectra; in **11a** the two methyl groups attached to silicon are related by a rotation about the Fe–Si axis, whereas they are inequivalent in **11b**. bis(1,2,4,5,6,7-Hexamethylindenyl)iron **8** was synthesised as a reference compound by the reaction of lithium 1,2,4,5,6,7-hexamethylindenide and $FeCl_2 \cdot 1.5THF$; this compound was also obtained as a mixture of diastereomers.

3.2. Characterisation of $Fe(\eta^5\text{-}C_9Me_6)_2SiMe_2$, 11

The monomeric nature of **11** was indicated by its FAB mass spectrum, which showed the parent ion with $m/z = 510$. The FAB mass spectrum also showed species arising from reaction of **11** with the matrix; the alcoholysis product $Fe(\eta^5\text{-}C_9Me_6H)(\eta^5\text{-}C_9Me_6SiMe_2\text{-}OR)$ (R = 3-nitrobenzyl) and the hydrolysis products $Fe(\eta^5\text{-}C_9Me_6H)(\eta^5\text{-}C_9Me_6SiMe_2OH)$ and $\{Fe(\eta^5\text{-}C_9Me_6H)(\eta^5\text{-}C_9Me_6SiMe_2)\}_2O$. The formation of such species is typical of strained [1]-ferrocenophanes [2]. We have also found that reaction of **11** and methanol gives the alcoholysis product $Fe(\eta^5\text{-}C_9Me_6H)(\eta^5\text{-}C_9Me_6\text{-}SiMe_2OMe)$.

The ^{13}C NMR spectrum of **11** also provides evidence for the strained ring-tilted structure; the resonances assigned to the *ipso* bridgehead carbons are found at chemical shifts (δ in C_6D_6) of 21.7 (**11a**) and 20.3 ppm (**11b**). These are very low chemical shifts for formally sp^2 carbon atoms; similar effects have been observed in other [1]-ferrocenophanes and reflect the distortion of the *ipso* carbon geometry from planarity. However, the shifts for **11** are the lowest recorded for a silicon-bridged ferrocenophane (cf. 33.5, 32.2, 27.5/33.5 and 25.6 ppm for **1**, **2**, **3** and **4** respectively); this is probably due to both the electron richness of **11** and the large distortion of the *ipso* carbon from planarity (β) shown by the crystal structure (vide infra).

The position of the visible absorption feature of ferrocene systems referred to as band II, which corresponds to two spin-allowed d–d transitions [39], has been found to be a good indicator of ring tilt [40]. For example, the band II absorptions of species such as $Fe(\eta^5\text{-}C_5H_4)_2SiMe_2$ [13] and $Fe(\eta^5\text{-}C_5H_4)_2(CMe_2)_2$ [40], both with appreciable ring tilts, show substantial red shifts relative to those of non-bridged analogues, whereas the essentially untilted [4]-ferrocenophane $Fe(\eta^5\text{-}C_5H_4)_2(CH_2)_4$ has a very similar UV–vis spectrum to 1,1′-diethylferrocene [40]. A similar effect is operative in the bis(indenyl) iron compounds, as can be seen by comparing the UV–vis spectra in THF of **8** (isomeric mixture) and **11** (spectra of pure **11a** and an isomeric mixture are essentially identical). The major difference between the spectra is the position of the second lowest energy band: for **8** this band is characterised by λ_{max} = ca. 425 nm, whereas that for **11** has λ_{max} = ca. 470 nm.

[1]-Ferrocenophanes have previously been shown to exhibit unusual ^{57}Fe Mössbauer spectra, with reduced isomer shifts (δ) and quadrupolar splittings (ΔE_q) relative to unbridged analogues [13,41,42]. These results have been interpreted in terms of Fe–Si interactions; density functional calculations suggest these interactions involve full Si–C bonding orbitals overlapping with empty metal e* orbitals [14]. We have therefore recorded ^{57}Fe Mössbauer data for **8** and **11a** to see whether a similar effect is present in bridged bis(indenyl)iron species. The values of δ and ΔE_q are presented in Table 2, together with data for other $SiMe_2$-bridged [1]-ferrocenophanes and their unbridged analogues. It can be seen that the indenyl compounds show increased isomer shifts relative to the cyclopentadienyl compounds; this feature presumably reflects the differences between the bonding in the two classes of compounds. Significant differences between bonding in indenyl and cyclopentadienyl complexes have previously been revealed by photoelectron spectroscopy [27,43]. **11a** also shows a greatly reduced isomer shift and quadrupolar splitting relative to **8**, indicating that similar Fe–Si interactions to those proposed for other [1]-ferrocenophanes may be operative.

The $SiMe_2$-bridged ferrocenophanes **1**–**4** have previously been found to exhibit electrochemically reversible oxidations at similar potentials to their unbridged analogues (0.00, −0.10, −0.21 and −0.39 V respectively

Table 2
^{57}Fe Mössbauer data for some [1]-ferrocenophanes and their unbridged analogues

Compound	δ (mm s^{-1})	ΔE_q (mm s^{-1})	T (K)	Fe–Si (Å)	Ref.
$Fe(\eta^5\text{-}C_5H_5)_2$	0.44	2.37	295		[45]
1	0.38	1.92	298	2.690(3)	[13]
$Fe(\eta^5\text{-}C_5Me_4H)_2$	0.44	2.51	293		[46]
4	0.36	1.85	298	2.652(1)	[13]
8	0.54	2.55	298		this work
11a	0.49	2.01	298	2.633(2)	this work

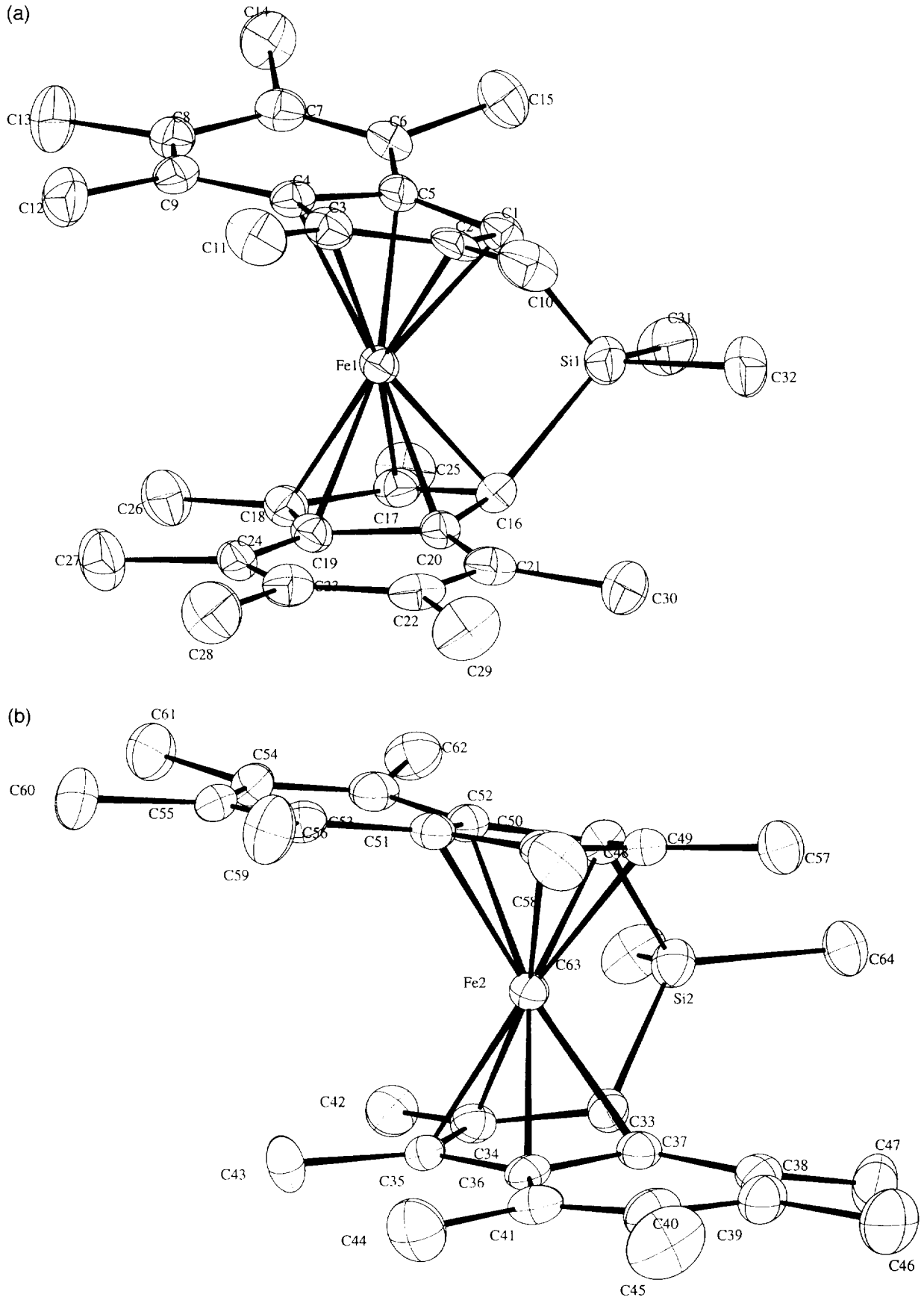

Fig. 2. Views of the two molecules (a) **11a**′ and (b) **11a**″ in the asymmetric unit of the crystal structure of **11a** showing the atomic labelling scheme and 50% thermal probability ellipsoids (H atoms excluded for clarity).

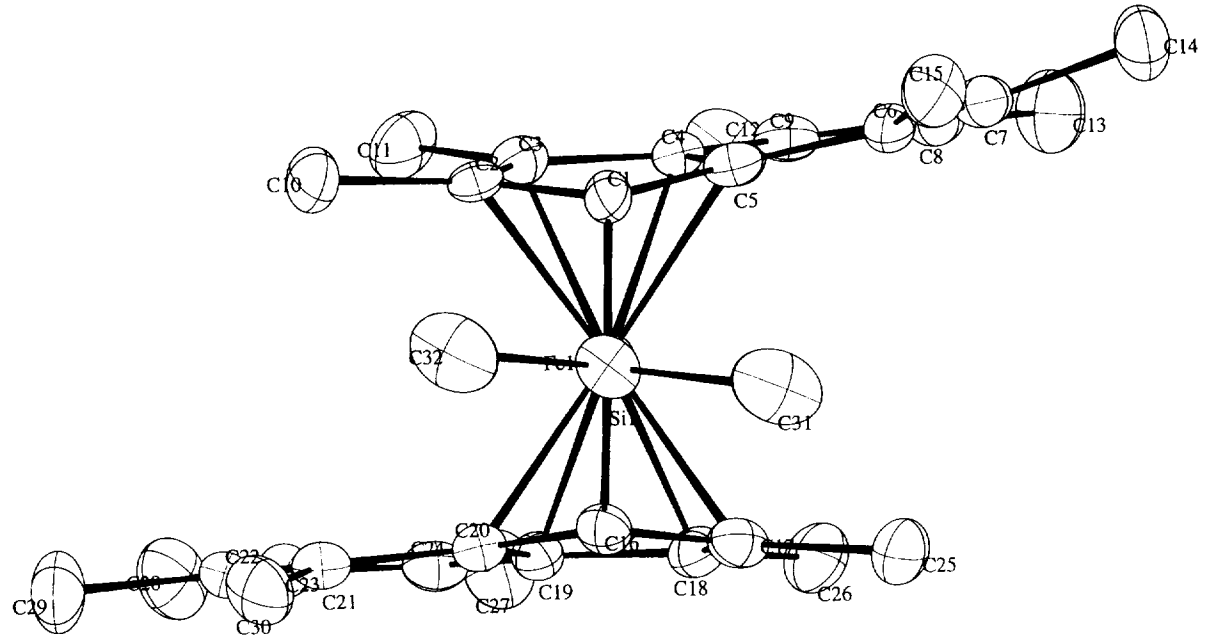

Fig. 3. A view of the molecular structure of **11a'** in the crystal structure of **11a** along the Si(1)–Fe(1) vector.

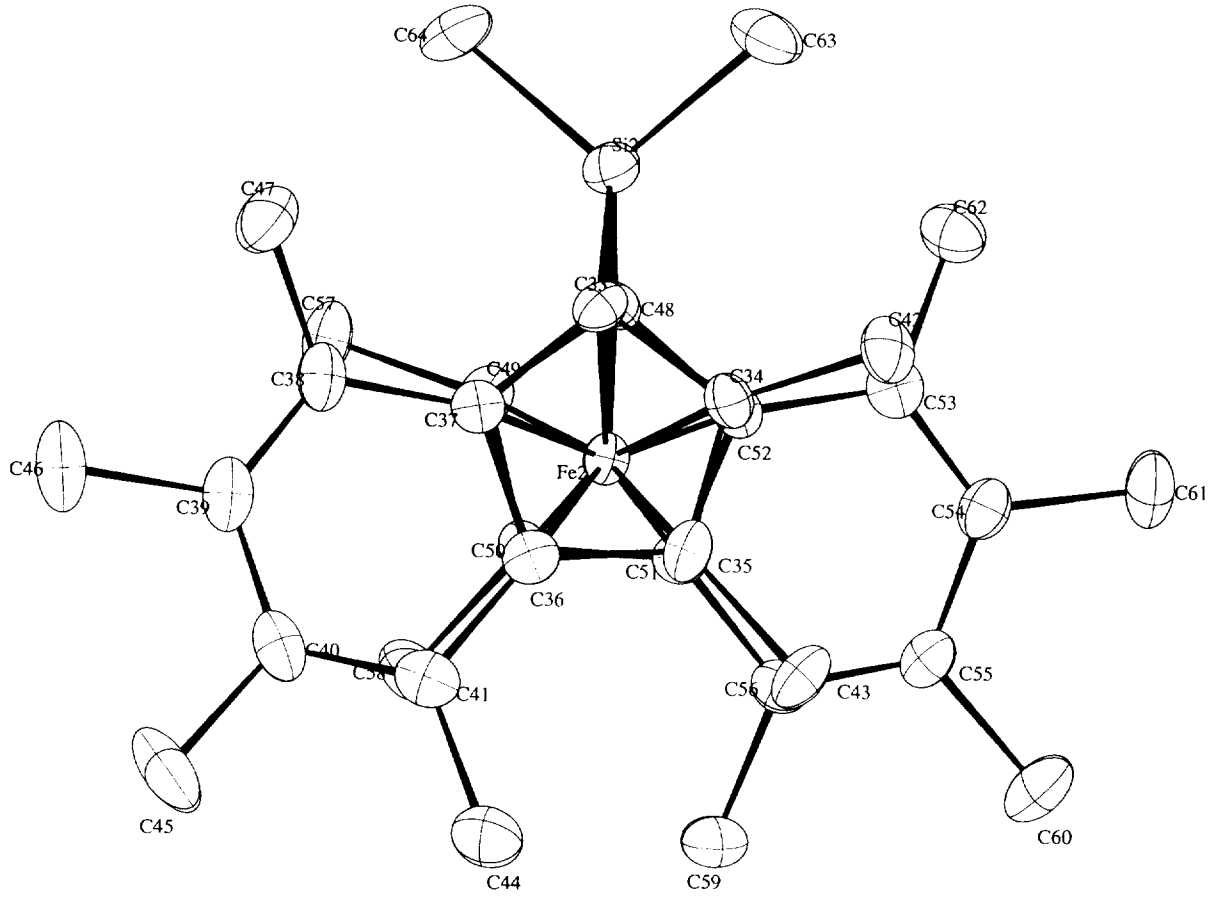

Fig. 4. A view of the molecular structure of **11a'** in the crystal structure of **11a** viewed through the centroids of the C_5-rings of the indenyl ligands.

Table 3
Fractional atomic coordinates and equivalent isotropic temperature factors (U_{eq} = one-third of the trace of the orthogonalised U_{ij} tensor) for **11a**. (The two independent molecules in the asymmetric unit are denoted by ′ and ″)

Atom	x	y	z	U_{eq} (Å²)
Molecule 11a′				
Fe(1)	0.37886(5)	0.8056(1)	0.0936(1)	0.0313
Si(1)	0.2612(1)	0.6953(3)	−0.0613(2)	0.0449
C(1)	0.3023(4)	0.9006(8)	0.0929(7)	0.0338
C(2)	0.3713(4)	0.9448(8)	0.0856(8)	0.0322
C(3)	0.4215(4)	1.0174(9)	0.1950(8)	0.0398
C(4)	0.3847(4)	1.0304(8)	0.2779(7)	0.0339
C(5)	0.3109(4)	0.9696(8)	0.2214(7)	0.0327
C(6)	0.2588(4)	0.9964(8)	0.2986(8)	0.0346
C(7)	0.2818(4)	1.0643(9)	0.4173(8)	0.0431
C(8)	0.3567(4)	1.0989(8)	0.4630(7)	0.0407
C(9)	0.4071(4)	1.0909(8)	0.4009(8)	0.0392
C(10)	0.3902(5)	0.924(1)	−0.0180(9)	0.0514
C(11)	0.4986(4)	1.074(1)	0.2117(9)	0.0558
C(12)	0.4870(5)	1.137(1)	0.4493(9)	0.0610
C(13)	0.3787(5)	1.153(1)	0.5870(8)	0.0620
C(14)	0.2289(5)	1.113(1)	0.5097(8)	0.0572
C(15)	0.1809(4)	0.976(1)	0.2565(9)	0.0529
C(16)	0.3322(4)	0.5937(8)	−0.0718(7)	0.0355
C(17)	0.3388(4)	0.6164(8)	0.0331(7)	0.0384
C(18)	0.4122(4)	0.6614(8)	0.0888(7)	0.0389
C(19)	0.4543(4)	0.6564(8)	0.0145(7)	0.0342
C(20)	0.4063(4)	0.6097(8)	−0.0870(7)	0.0330
C(21)	0.4363(5)	0.5808(9)	−0.1839(8)	0.0413
C(22)	0.5084(5)	0.6114(9)	−0.1726(8)	0.0407
C(23)	0.5554(4)	0.6700(9)	−0.0642(8)	0.0421
C(24)	0.5299(4)	0.6877(8)	0.0240(8)	0.0369
C(25)	0.2792(4)	0.593(1)	0.0787(9)	0.0536
C(26)	0.4346(5)	0.702(1)	0.2066(8)	0.0549
C(27)	0.5788(4)	0.742(1)	0.1342(9)	0.0591
C(28)	0.6350(4)	0.705(1)	−0.0558(9)	0.0648
C(29)	0.5418(5)	0.585(1)	−0.2715(9)	0.0661
C(30)	0.3887(5)	0.501(1)	−0.3070(8)	0.0542
C(31)	0.1718(4)	0.637(1)	−0.055(1)	0.0649
C(32)	0.2395(5)	0.655(1)	−0.2015(9)	0.0678
Molecule 11a″				
Fe(2)	0.14383(6)	0.5564(1)	0.3659(1)	0.0301
Si(2)	0.2543(1)	0.5194(3)	0.4418(2)	0.0409
C(33)	0.1660(4)	0.5914(9)	0.5103(7)	0.0341
C(34)	0.1027(4)	0.4797(8)	0.4248(7)	0.0334
C(35)	0.0498(4)	0.5407(8)	0.4155(7)	0.0329
C(36)	0.0741(4)	0.6983(9)	0.5046(7)	0.0328
C(37)	0.1441(4)	0.7294(9)	0.5651(7)	0.0334
C(38)	0.1800(4)	0.8850(9)	0.6693(7)	0.0372
C(39)	0.1503(5)	0.9924(9)	0.6942(8)	0.0482
C(40)	0.0825(5)	0.9604(9)	0.6282(8)	0.0472
C(41)	0.0431(4)	0.818(1)	0.5381(8)	0.0413
C(42)	0.0918(4)	0.3203(9)	0.3555(8)	0.0441
C(43)	−0.0211(4)	0.447(1)	0.3265(8)	0.0485
C(44)	−0.0313(5)	0.782(1)	0.4750(9)	0.0610
C(45)	0.0538(6)	1.087(1)	0.663(1)	0.0708
C(46)	0.1881(5)	1.158(1)	0.8019(9)	0.0662
C(47)	0.2440(5)	0.929(1)	0.7576(8)	0.0570
C(48)	0.2385(4)	0.4841(8)	0.3017(7)	0.0336
C(49)	0.2312(4)	0.6170(9)	0.3381(7)	0.0368
C(50)	0.1689(4)	0.5940(9)	0.2696(7)	0.0334
C(51)	0.1385(4)	0.4391(9)	0.1765(7)	0.0323
C(52)	0.1808(4)	0.3695(8)	0.1919(7)	0.0309
C(53)	0.1661(4)	0.2069(9)	0.0999(8)	0.0397
C(54)	0.1063(4)	0.1281(9)	0.0098(7)	0.0394
C(55)	0.0601(4)	0.2006(9)	0.0008(7)	0.0359
C(56)	0.0755(4)	0.3514(9)	0.0783(7)	0.0367
C(57)	0.2838(4)	0.7652(9)	0.4358(8)	0.0500
C(58)	0.1453(5)	0.716(1)	0.2925(9)	0.0538
C(59)	0.0323(5)	0.428(1)	0.0641(9)	0.0559
C(60)	−0.0070(5)	0.103(1)	−0.1001(8)	0.0586
C(61)	0.0886(5)	−0.0428(9)	−0.0888(8)	0.0547
C(62)	0.2192(4)	0.1269(9)	0.0976(8)	0.0485
C(63)	0.2713(5)	0.357(1)	0.4033(8)	0.0532
C(64)	0.3376(4)	0.653(1)	0.5523(8)	0.0519

vs. ferrocenium/ferrocene in dichloromethane). We recorded the cyclic voltammogram of **11** (as an isomeric mixture) in dichloromethane and found a reversible oxidation at −0.64 V vs. ferrocenium/ferrocene, showing **11** to be very electron rich. This value can be

Table 4
Selected bond lengths (Å) for **11a**

Molecule 11a′			
Fe(1)–Si(1)	2.614(2)	C(3)–C(4)	1.42(1)
Fe(1)–C(1)	2.002(7)	C(4)–C(5)	1.44(1)
Fe(1)–C(2)	2.023(7)	C(4)–C(9)	1.46(1)
Fe(1)–C(3)	2.042(8)	C(5)–C(6)	1.44(1)
Fe(1)–C(4)	2.062(7)	C(6)–C(7)	1.36(1)
Fe(1)–C(5)	2.093(7)	C(7)–C(8)	1.44(1)
Fe(1)–C(16)	2.002(7)	C(8)–C(9)	1.36(1)
Fe(1)–C(17)	2.039(7)	C(16)–C(17)	1.45(1)
Fe(1)–C(18)	2.057(7)	C(16)–C(20)	1.47(1)
Fe(1)–C(19)	2.079(7)	C(17)–C(18)	1.44(1)
Fe(1)–C(20)	2.059(7)	C(18)–C(19)	1.42(1)
Si(1)–C(1)	1.901(8)	C(19)–C(20)	1.45(1)
Si(1)–C(16)	1.906(8)	C(19)–C(24)	1.44(1)
Si(1)–C(31)	1.872(9)	C(20)–C(21)	1.43(1)
Si(1)–C(32)	1.872(9)	C(21)–C(22)	1.37(1)
C(1)–C(2)	1.46(1)	C(22)–C(23)	1.45(1)
C(1)–C(5)	1.46(1)	C(23)–C(24)	1.35(1)
C(2)–C(3)	1.43(1)		
Molecule 11a″			
Fe(2)–Si(2)	2.633(2)	C(35)–C(36)	1.43(1)
Fe(2)–C(33)	1.990(7)	C(36)–C(37)	1.44(1)
Fe(2)–C(34)	2.027(7)	C(36)–C(41)	1.45(1)
Fe(2)–C(35)	2.046(7)	C(37)–C(38)	1.45(1)
Fe(2)–C(36)	2.088(7)	C(38)–C(39)	1.36(1)
Fe(2)–C(37)	2.054(7)	C(39)–C(40)	1.44(1)
Fe(2)–C(48)	2.006(7)	C(40)–C(41)	1.38(1)
Fe(2)–C(49)	2.028(7)	C(48)–C(49)	1.45(1)
Fe(2)–C(50)	2.034(7)	C(48)–C(52)	1.48(1)
Fe(2)–C(51)	2.072(7)	C(49)–C(50)	1.42(1)
Fe(2)–C(52)	2.062(7)	C(50)–C(51)	1.42(1)
Si(2)–C(33)	1.905(8)	C(51)–C(52)	1.43(1)
Si(2)–C(48)	1.905(7)	C(51)–C(56)	1.46(1)
Si(2)–C(63)	1.858(8)	C(52)–C(53)	1.45(1)
Si(2)–C(64)	1.863(8)	C(53)–C(54)	1.37(1)
C(33)–C(34)	1.46(1)	C(54)–C(55)	1.44(1)
C(33)–C(37)	1.45(1)	C(55)–C(56)	1.37(1)
C(34)–C(35)	1.41(1)		

Table 5
Selected bond angles (°) for **11a**

Molecule 11a'		*Molecule 11a''*	
C(1)–Si(1)–C(16)	99.2(3)	C(33)–Si(2)–C(48)	98.2(3)
C(1)–Si(1)–C(31)	116.3(4)	C(33)–Si(2)–C(63)	112.3(4)
C(16)–Si(1)–C(31)	110.5(4)	C(48)–Si(2)–C(63)	118.6(4)
C(1)–Si(1)–C(32)	112.1(4)	C(33)–Si(2)–C(64)	117.2(4)
C(16)–Si(1)–C(32)	119.0(4)	C(48)–Si(2)–C(64)	111.3(4)
C(31)–Si(1)–C(32)	100.5(5)	C(63)–Si(2)–C(64)	100.3(4)
Si(1)–C(1)–C(5)	122.8(5)	Si(1)–C(1)–C(2)	115.6(5)
C(2)–C(1)–C(5)	103.8(6)	Si(2)–C(33)–C(34)	115.4(5)
C(1)–C(2)–C(3)	110.3(7)	Si(2)–C(33)–C(37)	123.8(5)
C(2)–C(3)–C(4)	107.7(7)	C(34)–C(33)–C(37)	103.5(6)
C(3)–C(4)–C(5)	107.8(7)	C(33)–C(34)–C(35)	110.7(6)
C(3)–C(4)–C(9)	133.1(7)	C(34)–C(35)–C(36)	108.1(6)
C(5)–C(4)–C(9)	119.0(7)	C(35)–C(36)–C(37)	106.6(7)
C(1)–C(5)–C(4)	109.6(7)	C(35)–C(36)–C(41)	133.1(7)
C(1)–C(5)–C(6)	131.0(7)	C(37)–C(36)–C(41)	120.3(7)
C(4)–C(5)–C(6)	119.1(7)	C(33)–C(37)–C(36)	110.6(7)
C(5)–C(6)–C(7)	118.9(7)	C(33)–C(37)–C(38)	130.4(7)
C(6)–C(7)–C(8)	121.7(7)	C(36)–C(37)–C(38)	119.0(7)
C(7)–C(8)–C(9)	121.0(7)	C(37)–C(38)–C(39)	118.5(8)
C(4)–C(9)–C(8)	118.7(7)	C(38)–C(39)–C(40)	122.6(8)
Si(1)–C(16)–C(17)	115.1(5)	C(39)–C(40)–C(41)	120.6(8)
Si(1)–C(16)–C(20)	122.2(5)	C(36)–C(41)–C(40)	118.4(8)
C(17)–C(16)–C(20)	104.0(6)	Si(2)–C(48)–C(49)	116.3(5)
C(16)–C(17)–C(18)	110.4(6)	Si(2)–C(48)–C(52)	122.2(5)
C(17)–C(18)–C(19)	107.9(7)	C(49)–C(48)–C(52)	103.0(6)
C(18)–C(19)–C(20)	107.6(6)	C(48)–C(49)–C(50)	111.4(6)
C(18)–C(19)–C(24)	132.6(7)	C(49)–C(50)–C(51)	107.3(7)
C(20)–C(19)–C(24)	119.8(7)	C(50)–C(51)–C(52)	108.2(7)
C(16)–C(20)–C(19)	109.7(6)	C(50)–C(51)–C(56)	131.4(7)
C(16)–C(20)–C(21)	131.7(7)	C(52)–C(51)–C(56)	120.4(7)
C(19)–C(20)–C(21)	118.6(7)	C(48)–C(52)–C(51)	109.6(6)
C(20)–C(21)–C(22)	120.1(7)	C(48)–C(52)–C(53)	130.5(7)
C(20)–C(21)–C(30)	119.8(7)	C(51)–C(52)–C(53)	119.7(7)
C(22)–C(21)–C(30)	119.8(7)	C(52)–C(53)–C(54)	118.2(7)
C(21)–C(22)–C(23)	120.6(7)	C(53)–C(54)–C(55)	122.0(7)
C(22)–C(23)–C(24)	121.2(7)	C(54)–C(55)–C(56)	121.6(7)
C(19)–C(24)–C(23)	119.4(7)	C(51)–C(56)–C(55)	117.6(7)

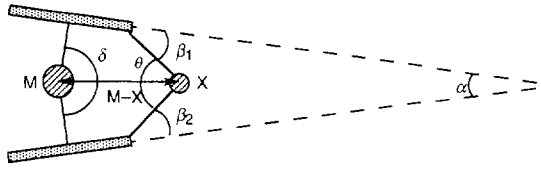

Fig. 5. Some parameters used in the discussion of the structures of [1]-metallocenophanes.

compared with -0.69 V for the unbridged model compound **8**.

3.3. Crystal structure of rac-Fe(C_9Me_6)$_2$SiMe$_2$, 11a

Single crystals of the *rac*-diastereomer **11a** of Fe(η^5-C_9-Me_6)$_2$SiMe$_2$ were obtained by slow cooling of a pentane solution of a mixture of **11a** and **11b**. The crystal structure was solved and refined in the centrosymmetric space group $P\bar{1}$, with two independent molecules in the asymmetric unit; these are denoted **11a'** and **11a''** and are shown in Fig. 2(a) and 2(b) respectively. Figs. 3 and 4 show additional views of the molecular structure of **11a'**. Fractional atomic coordinates and equivalent isotropic temperature factors for the non-hydrogen atoms are given in Table 3, whilst selected bond lengths and angles appear in Tables 4 and 5 respectively. Fig. 5 defines some parameters which have been used in discussion of [1]-ferrocenophane structures; Table 6 compares these parameters for **11a'** and **11a''** with those for **1** [6], **2** [13] and **4** [13], the other SiMe$_2$-bridged [1]-ferrocenophanes to have been studied crystallographically.

The Fe–C bond lengths range over similar values to other [1]-ferrocenophanes [6,9,10,12,13,18]. In common with other examples, the shortest bonds are those to the *ipso* bridgehead carbons. The longest Fe–C bonds are those to the carbons at the ring junctions of the five- and six-membered rings. This feature is typical of metal η^5-indenyl structures; representative examples include bis(η^5-heptamethylindenyl)iron (short distances 2.058(4)–2.066 (3) Å; long distances 2.086(4)–2.098(4) Å) [46], bis(η^5-1,3-dimethylindenyl)iron hexafluorophosphate (2.063(4)–2.079(4) Å; 2.142(4)–2.156(4) Å) [47], (η^5-indenyl)Rh(η^4-norbornadiene) (2.224(5)–2.240(5) Å; 2.388(3)–2.401(3) Å) [48] and (η^5-heptamethylindenyl)titanium trichloride (2.352(4)–2.360(4) Å; 2.383(4)–2.400(4) Å) [49]. The bond length alternation in the six-membered rings is also typical of η^5-indenyl species [46–49].

Both **11a'** and **11a''** show considerably smaller ring tilt angles α (defined in Fig. 5) than any other silicon-bridged [1]-ferrocenophane to have previously been

Table 6
Comparison of structural data (parameters defined in Fig. 5) for SiMe$_2$-bridged [1]-ferrocenophanes

	1 [6]	**2** [13]	**4** [13]	**11a'**	**11a''**
α (°)	20.8	18.6	16.1	13.0	13.8
β (°) (av. of β_1 and β_2)	37.0	39.1	40.3	43.1	41.2
δ (°)	164.7	166.5	168.6	170.89	170.25
θ (°)	95.7(4)	97.0(1)	98.1(1)	99.2(3)	98.2(3)
Me–Si–Me (°)	114.8(6)	112.3(2)	103.2(1)	100.5(5)	100.3(4)
Si–*ipso* C (Å) (av.)	1.858(9)	1.884(3)	1.904(2)	1.904(8)	1.905(8)
Fe–Si (Å)	2.690(3)	2.6767(8)	2.652(1)	2.614(2)	2.633(2)

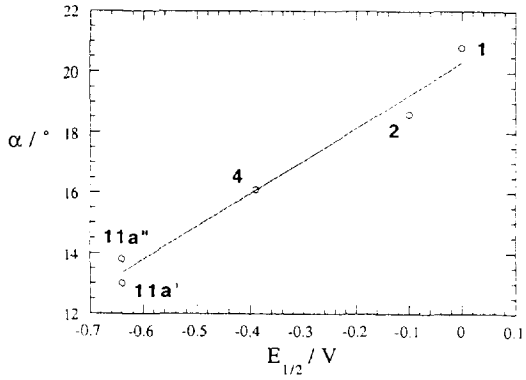

Fig. 6. Plot of the crystallographically determined ring tilt α vs. the electrochemical oxidation potential $E_{1/2}$ (in dichloromethane, vs. ferrocenium/ferrocene) for some $SiMe_2$-bridged [1]-ferrocenophanes.

structurally characterised. This necessarily requires greater distortion of the *ipso* carbon from planarity, i.e. an increase in β, and a decrease in the Fe–Si distance. The short distances between the iron and the bridging atoms of [1]-ferrocenophanes have been implicated as causes of the unusual Mössbauer spectra of these species [13,41,42,44]; interactions between Fe and Si orbitals have been revealed by density functional calculations for **1** [14]. The Fe–Si distances in Table 6 are a little greater than the sum of the covalent radii (2.37 Å) or than typical Fe–Si bonds (2.30–2.36 Å). The bridgehead C–Si bonds are typically greater in the $SiMe_2$-bridged [1]-ferrocenophanes than the Si–Me bonds. The discrepancy between bridgehead–Si and Me–Si bond lengths is especially large in **11a**, this is presumably related to the low ring tilt

Comparison with other $SiMe_2$-bridged species (Table 5) reveals a trend whereby the most electron-rich species have lower ring tilts; this may be seen by a plot of ring tilt versus electrochemical oxidation potential (Fig. 6). Although the differences between the ring tilts of **1**, **4** and **11a** could be accounted for by a steric argument, i.e. minimising interference between the 2 and 2′ and between the 5 and 5′ substituents, the decreased ring tilt of **2** relative to **1** actually brings the two substituents closer to one another, thus indicating an electronic origin for the trend in ring tilt. Another interesting feature of the structure of **11a** is shown (for **11a′**) in Fig. 4; the coordination about the bridging silicon atom is distorted so the methyl susbtituents bend away from the six-membered rings of the indenyl groups.

4. Conclusions

We have developed a route to a new permethylated bridged indene ligand, which has been used to synthesise the first strained bridged bis(indenyl)iron complex $Fe(\eta^5\text{-}C_9Me_6)_2SiMe_2$ **11**. This iron complex has been shown by cyclic voltammetry to be very electron rich. The crystal structure of the *rac*-isomer reveals the lowest ring tilt found so far for a silicon-bridged [1]-ferrocenophane, and the greatest distortion from planarity at the bridgehead carbon atoms. ^{57}Fe Mössbauer spectra of **11** show reduced isomer shifts and quadrupolar splitting relative to the unbridged analogue $Fe(C_9Me_6H)_2$ **8**. Polymerisation studies are currently being conducted on **11**.

Acknowledgements

We thank the EPSRC mass spectrometry service for the FAB mass spectra and the EPSRC for support. S.B. also thanks the EPSRC for studentships, J.S.T. thanks the EPSRC and Shell plc for a CASE studentship and R.T.P. thanks NSERC (Canada) for a graduate scholarship.

References

[1] A.G. Osborne and R.H. Whiteley, *J. Organomet. Chem.*, *101* (1975) C27–C28.
[2] A.B. Fischer, J.B. Kinney, R.H. Staley and M.S. Wrighton, *J. Am. Chem. Soc.*, *101* (1979) 6501–6506.
[3] D. Seyferth and H.P. Withers, *Organometallics*, *1* (1982) 1275–1282.
[4] H.P. Withers, D. Seyferth, J.D. Fellman, P.E. Garrou and S. Martin, *Organometallics*, *1* (1982) 1283–1288.
[5] D.A. Foucher, B.-Z. Tang and I. Manners, *J. Am. Chem. Soc.*, *114* (1992) 6246–6248.
[6] W. Finckh, B.-Z. Tang, D.A. Foucher, D.B. Zamble, R. Ziembinski, A.J. Lough and I. Manners, *Organometallics*, *12* (1993) 823–829.
[7] D.A. Foucher, R. Ziembinski, B.-Z. Tang, P.M. Macdonald, J. Massey, C.R. Jaeger, G.J. Vansco and I. Manners, *Macromolecules*, *26* (1993) 2878–2884.
[8] D. Foucher, R. Ziembinski, R. Petersen, J. Pudelski, M. Edwards, Y.Z. Ni, J. Massey, C.R. Jaeger, G.J. Vansco and I. Manners, *Macromolecules*, *27* (1994) 3992–3999.
[9] D.A. Foucher, A.J. Lough, I. Manners, J. Rasburn and J.G. Vansco, *Acta Crystallogr.*, *C51* (1995) 580–582.
[10] J.K. Pudelski, R. Rulkens, D.A. Foucher, A.J. Lough, P.M. Macdonald and I. Manners, *Macromolecules*, *28* (1995) 7301–7308.
[11] M.T. Nguyen, A.F. Diaz, V.V. Dement'ev and K.H. Pannell, *Chem. Mater.*, *5* (1993) 1389–1394.
[12] K.H. Pannell, V.V. Dementiev, H. Li, F. Cervantes-Lee, M.T. Nguyen and A.F. Diaz, *Organometallics*, *13* (1994) 3644–3650.
[13] J.K. Pudelski, D.A. Foucher, C.H. Honeyman, A.J. Lough, I. Manners, S. Barlow and D. O'Hare, *Organometallics*, *14* (1995) 2470–2479.
[14] S. Barlow, M.J. Drewitt, J.C. Green, I. Manners, J.M. Nelson, D. O'Hare, J.K. Pudelski, C. Whittington and H. Wynn, in preparation.
[15] J.K. Pudelski, D.A. Foucher, P.M. Macdonald, C.H. Honeyman, I. Manners, S. Barlow and D. O'Hare, *Macromolecules*, *29* (1996) 1894–1903.

[16] D.A. Foucher and I. Manners, *Makromol. Chem., Rapid Commun., 14* (1993) 63–66.
[17] D.A. Foucher, M. Edwards, R.A. Burrow, A.J. Lough and I. Manners, *Organometallics, 13* (1994) 4959–4966.
[18] C.H. Honeyman, D.A. Foucher, F.Y. Dahmen, R. Rulkens, A.J. Lough and I. Manners, *Organometallics, 14* (1995) 5503–5512.
[19] J.K. Pudelski, D.P. Gates, R. Rulkens, A.J. Lough and I. Manners, *Angew. Chem., Int. Ed. Engl., 107* (1995) 1633–1635.
[20] J.M. Nelson, H. Rengel and I. Manners, *J. Am. Chem. Soc., 115* (1993) 7035–7036.
[21] J.M. Nelson, A.J. Lough and I. Manners, *Angew. Chem., Int. Ed. Engl., 33* (1994) 989–991.
[22] R. Rulkens, Y.Z. Ni and I. Manners, *J. Am. Chem. Soc., 116* (1994) 12121–12122.
[23] R. Rulkens, A.J. Lough and I. Manners, *J. Am. Chem. Soc., 116* (1994) 797–798.
[24] J. Rasburn, R. Petersen, T. Jahr, R. Rulkens, I. Manners and G.J. Vansco, *Chem. Mater., 7* (1995) 871–877.
[25] Y. Ni, R. Rulkens, J.K. Pudelski and I. Manners, *Makromol. Chem., Rapid Commun., 14* (1995) 637–641.
[26] N.P. Reddy, H. Yamashita and M. Tanaka, *J. Chem. Soc., Chem. Commun.*, (1995) 2263–2264.
[27] D. O'Hare, J.C. Green, T. Marder, S. Collins, G. Stringer, A.K. Kakkar, N. Kaltsoyannis, A. Kuhn, R. Lewis, C. Mehnert, P. Scott, M. Kurmoo and S. Pugh, *Organometallics, 11* (1992) 48–55.
[28] A. Altomare, G. Cascarano, C. Giacovazzo, A. Guagliardi, G. Polidori, M.C. Burla and M. Camalli, *J. Appl. Cryst., 27* (1994) 425.
[29] N. Walker and D. Stuart, *Acta Crystallogr., A39* (1983) 159–166.
[30] J.R. Carruthers and D.W. Watkin, *Acta Crystallogr., A35* (1979) 698.
[31] A.C. Larson, *Acta Crystallogr., 23* (1967) 664–665.
[32] J.R. Carruthers and D.J. Watkin, CRYSTALS, *User Manual*, Oxford University Computing Centre, Oxford, UK, 1975.
[33] J. Park, Y. Seo, S. Cho, D. Whang, K. Kim and T. Chang, *J. Organomet. Chem., 489* (1995) 23–25.
[34] M. Herberhold, *Angew. Chem., Int. Ed. Engl., 34* (1995) 1837–1839.
[35] M. Herberhold and T. Bärtl, *Z. Naturforsch, 50B* (1995) 1692–1698.
[36] K.L. Rinehart, A.K. Frerichs, P.A. Kittle, L.F. Westman, D.H. Gustafson, R.L. Pruett and J.E. McMahon, *J. Am. Chem. Soc., 82* (1960) 4111–4112.
[37] C.M. Fendrick, E.A. Mintz, L.D. Schertz, T.J. Marks and V.W. Day, *Organometallics, 3* (1984) 819–821.
[38] C.M. Fendrick, L.D. Schertz, V.W. Day and T.J. Marks, *Organometallics, 7* (1988) 1828–1838.
[39] Y.S. Sohn, D.N. Hendrickson and H.B. Gray, *J. Am. Chem. Soc., 93* (1971) 3603–3612 and references cited therein.
[40] T.H. Barr and W.E. Watts, *J. Organomet. Chem., 15* (1968) 177–185.
[41] J. Silver, *J. Chem. Soc., Dalton Trans.*, (1990) 3513–3516.
[42] M. Clemance, R.M.G. Roberts and J. Silver, *J. Organomet. Chem., 243* (1983) 461–467.
[43] N.S. Crossley, J.C. Green, A. Nagy and G. Stringer, *J. Chem. Soc., Dalton Trans.*, (1989) 2139–2147.
[44] A.G. Osborne, R.H. Whiteley and R.E. Meads, *J. Organomet. Chem., 193* (1980) 345–357.
[45] J.S. Miller, D.T. Glatzhofer, D.M. O'Hare, W.M. Reiff, A. Chakraborty and A.J. Epstein, *Inorg. Chem., 28* (1989) 2930–2939.
[46] S.A. Westcott, A.K. Kakkar, G. Stringer, N.J. Taylor and T.B. Marder, *J. Organomet. Chem., 394* (1990) 777–794.
[47] P.M. Treichel, J.W. Johnson and J.C. Calabrese, *J. Organomet. Chem., 88* (1975) 215–225.
[48] C. Bonifaci, A. Ceccon, A. Gambaro, P. Ganis, S. Santi, G. Valle and A. Venzo, *Organometallics, 12* (1993) 4211–4214.
[49] D. O'Hare, V. Murphy, G.M. Diamond, P. Arnold and P. Mountford, *Organometallics, 13* (1994) 4689–4694.